

Spin-dependent electron many-body effects in GaAs

P. Nemeč,* Y. Kerachian, and H. M. van Driel

Department of Physics and Institute for Optical Sciences, University of Toronto, Toronto, Canada M5S 1A7

Arthur L. Smirl

Laboratory for Photonics & Quantum Electronics, 138 IATL, University of Iowa, Iowa City, Iowa 52242, USA

(Received 11 August 2005; published 1 December 2005)

Time- and polarization-resolved differential transmission measurements employing same and oppositely circularly polarized 150 fs optical pulses are used to investigate spin characteristics of conduction band electrons in bulk GaAs at 295 K. Electrons and holes with densities in the $2 \times 10^{16} \text{ cm}^{-3}$ – 10^{18} cm^{-3} range are generated and probed with pulses whose center wavelength is between 865 and 775 nm. The transmissivity results can be explained in terms of the spin sensitivity of both phase-space filling and many-body effects (band-gap renormalization and screening of the Coulomb enhancement factor). For excitation and probing at 865 nm, just above the band-gap edge, the transmissivity changes mainly reflect spin-dependent phase-space filling which is dominated by the electron Fermi factors. However, for 775 nm probing, the influence of many-body effects on the induced transmission change are comparable with those from reduced phase space filling, exposing the spin dependence of the many-body effects. If one does not take account of these spin-dependent effects one can misinterpret both the magnitude and time evolution of the electron spin polarization. For suitable measurements we find that the electron spin relaxation time is 130 ps.

DOI: [10.1103/PhysRevB.72.245202](https://doi.org/10.1103/PhysRevB.72.245202)

PACS number(s): 78.47.+p, 72.25.Fe, 71.55.Eq

I. INTRODUCTION

Extensive investigations of free electrons and holes excited in GaAs via interband transitions by femtosecond laser pulses have provided us with considerable insight into the optical and electronic properties of nonequilibrium carriers.^{1,2} Both single particle and many-body electronic effects such as carrier thermalization, dephasing, cooling, and band-gap renormalization have now been well studied;³ optical effects including gain dynamics, local field effects, Coulomb enhancement of interband transitions are also reasonably well understood.⁴ However much of this research was carried out using linearly polarized pulses which provide little, if any, insight into carrier spin characteristics. Recently there has been growing interest in controlling the spin of electrons and holes in semiconductors^{5–7} with the goal of making spin-based devices in the burgeoning field of what has come to be known as spintronics. Many of the concepts surrounding active components in spintronics involve transport of free electrons in bulk and low dimensional semiconductors. Consequently, it is essential to understand how spin effects influence various optical and electronic properties of semiconductors. In this paper we illustrate how spin-dependent many-body effects manifest themselves in altering the optical transmission of GaAs at room temperature. As a corollary, we show how these many-body effects influence the interpretation of experiments which attempt to examine spin relaxation of conduction band electrons.

It has been known for nearly four decades that the optical excitation of direct band-gap zinc-blende and other semiconductors with above band-gap circularly polarized light creates spin-polarized electrons in the conduction band.^{8,9} From measurements of the differential transmission using pump-probe techniques with the same and oppositely circularly polarized pulses, or from photoluminescence¹⁰ measurements,

it is possible to establish the degree of carrier spin polarization and its decay time.^{8,11–14} Since the hole spin polarization in bulk semiconductors is known to relax¹⁵ in $\lesssim 100$ fs, on a longer time scale one typically measures only the electron spin polarization and its evolution. For optical excitation of zinc-blende semiconductors with photon energy just above the band gap, because of the selection rules⁸ governing optical transitions from heavy, or light hole, states to conduction band states, right circular polarization (σ^+) generates a density of spin-down electrons (N^\downarrow) which is $3 \times$ the density (N^\uparrow) of spin-up electrons, and vice versa for left circularly polarized light (σ^-). Hence the initial degree of electron spin polarization generated by a circularly polarized beam in a zinc-blende semiconductor, defined⁵ as $P = (N^\downarrow - N^\uparrow) / (N^\downarrow + N^\uparrow)$, is ± 0.5 .

For many of the femtosecond pump-probe experiments reported to date, electrons and holes are typically optically excited at low density and probed with linearly polarized light with photon energy, $\hbar\omega$, slightly higher than the band gap, E_g , for which the semiconductor transmissivity is dominated by phase space filling (PSF).¹ However, in pump-probe experiments where high densities ($> 10^{17} \text{ cm}^{-3}$ in GaAs) and/or large probe photon energies are involved, many-body effects such as band-gap renormalization (BGR) and alteration of the Sommerfeld-Coulomb enhancement factor (CEF), also referred to as the local field correction,¹⁸ are observed.^{4,16,17} Indeed, Langot *et al.*⁴ have conducted theoretical and experimental investigations of the relative roles of PSF and the combined BGR-CEF effects in GaAs at room temperature for carrier density $> 10^{17} \text{ cm}^{-3}$ and for probe photon energies with $\hbar\omega - E_g > 100 \text{ meV}$ where $E_g = 1.42 \text{ eV}$ at 295 K. However, because their experiments were conducted with linearly polarized light pulses, they could not provide insight into the influence of spin on many-body effects.

Here we report the results of femtosecond pump-probe differential transmission measurements in GaAs under conditions similar to that of Langot *et al.* but for same and oppositely circularly polarized beams. Experiments were conducted with 150 fs pump pulses in the range 865 nm (1.43 eV)–775 nm (1.6 eV) injecting carrier densities in the 2×10^{16} – 10^{18} cm $^{-3}$ range; the probe pulse had a center wavelength of 865, 800 (1.55 eV), or 775 nm. The experiments allow us to develop insight into the spin dependence of the combined CEF-BGR effects especially at the shorter probe wavelengths (probing higher electron kinetic energy) where PSF effects are much smaller than they are for near band-edge probing and are comparable to many-body effects in influencing the transmissivity. Because of the preferential coupling of σ^+ and σ^- polarized light to spin-down and spin-up electrons, any spin imbalance changes the CEF-BGR effect involving a particular conduction spin band and this appears in the differential transmission. An equally important conclusion to be drawn from our work is that for probe measurements with photon energy well above the band gap, the traditional approach of using differential transmission measurements for same and oppositely circularly polarized beams may not directly yield a measure of the net electron spin polarization or its relaxation time.

The remainder of this paper is organized as followed. In Sec. II, we discuss the theoretical background related to the optical transmission properties of spin-polarized electrons within an ambipolar plasma in a zinc-blende semiconductor and establish the formalism used to discuss our experimental results. Because of the inherent difficulty of calculating many-body carrier effects in semiconductors even for spin unpolarized degenerate carriers, for nondegenerate spin polarized carriers we will not attempt to explicitly calculate the magnitude of spin-dependent CEF-BGR effects here. Section III provides details of the experimental techniques for time- and polarization resolved pump-probe measurement. In Sec. IV, we present and discuss results of the differential transmission measurements for different pump and probe wavelengths and injected carrier densities and offer evidence for the spin-dependent many-body effects. The paper ends with some general but conservative conclusions about spin-dependent electron many-body effects and suggestions for future work.

II. THEORETICAL BACKGROUND

To illustrate how the presence of spin-dependent many-body effects can manifest themselves in polarization sensitive pump-probe transmission experiments we briefly outline the salient features of the optical response of a zinc-blende, direct gap, semiconductor such as GaAs. We begin by considering a semiconductor excited with linearly polarized light which generates a spin-unpolarized ambipolar plasma of density N . Figure 1 is a schematic diagram illustrating how a probe photon of energy $\hbar\omega > E_g$, but less than the spin-orbit split off gap, couples heavy hole (hh) and light hole (lh) states to conduction band (c) states. As shown elsewhere,^{2,4} the absorption coefficient experienced by a linearly polarized probe beam has the form

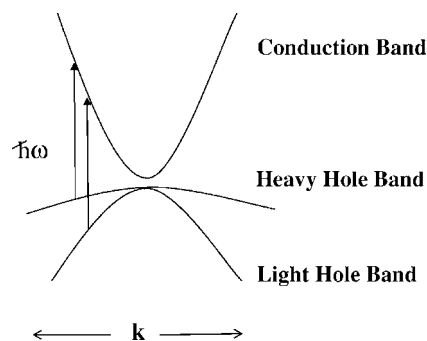


FIG. 1. Schematic diagram of interband transitions between light/heavy hole bands and conduction bands in bulk GaAs at photon energy $\hbar\omega > E_g$.

$$\alpha(\omega, N) = a_0 \sum_v \mu_v^{3/2} C_v(\omega, N) \sqrt{\Delta E(N)} [1 - f_v(k_v) - f_c(k_v)]. \quad (1)$$

Here $\nu = lh, hh$, and μ_ν is the reduced effective optical mass for valence band ν and the lowest conduction band, i.e., $\mu_\nu = m_c m_\nu / (m_c + m_\nu)$. For GaAs (Ref. 19) $m_c = 0.066m_0$, $m_{hh} = 0.5m_0$, $m_{lh} = 0.084m_0$ giving $\mu_{hh}^{3/2} / \mu_{lh}^{3/2} \approx 2$. The parameter k_v is the wave vector for the probed electron and hole bands which we assume to be parabolic so that $k_v = \sqrt{2\mu_\nu \Delta E} / \hbar$. The f_i are Fermi occupancy factors for band i and $\Delta E(N) = \hbar\omega - E_g(N)$. The $C_v(\omega, N)$ are CEF's² of the interband optical transitions. Many-body effects manifest themselves with increasing N and lead to, *inter alia*, band-gap renormalization (reduction) expressed through $E_g(N)$, and screening of the Coulomb field^{2,4} leading to a density dependence of the CEF. The quantity a_0 is a constant related to the strength of inter-band momentum matrix elements; for GaAs with $\hbar\omega \gtrsim E_g$, $\alpha(\omega, 0) \sim 10^6$ m $^{-1}$.

We now consider the situation where the pump and probe beams are circularly polarized so that spin-polarized electrons and unpolarized holes are being probed. We remind the reader that for electrons or holes near the band edge total electronic angular momentum, J , and its projection on a preferred axis, m_J , are good quantum numbers so that the heavy and light hole bands as well as the conduction band can be characterized by states $|J, m_J\rangle$. The hh states are given by $|3/2, \pm 3/2\rangle$, the lh states by $|3/2, \pm 1/2\rangle$, and the conduction band states by $|1/2, \pm 1/2\rangle$. For the conduction band, a zero orbital angular momentum band, m_J can be identified with spin-up and spin-down electron states, viz. $|\downarrow\rangle$ and $|\uparrow\rangle$, however, hh and lh bands have mixed spin character. When one considers all the band states at different wave vector, k , that can participate in optical transitions one finds that σ^+ polarized light generates $3 \times$ as many electrons in $|\downarrow\rangle$ states as in $|\uparrow\rangle$ states from *each of the* lh and hh hole bands, with the opposite occurring for σ^- light. Figure 2 illustrates these selection rules for $\hbar\omega \gtrsim E_g$ (i.e., for $k_v \approx 0$); these selection rules, or at least the relative transition rates, are relaxed somewhat when $\hbar\omega$ approaches the spin-orbit split-off energy gap.^{8,9}

For a zinc-blende semiconductor which has been optically excited to produce a density N^\uparrow of spin-up electrons and

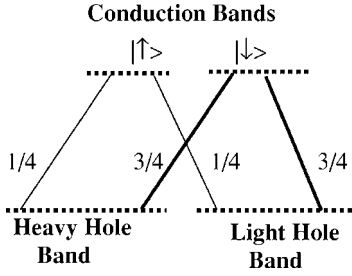


FIG. 2. Schematic diagram of transitions between heavy hole/light hole bands and $|\uparrow\rangle$ and $|\downarrow\rangle$ conduction band states indicating the relative transition strengths for σ^+ light; the 1/4, 3/4 ratios are interchanged for σ^- light.

density N^\downarrow of spin-down electrons with $N=N^\uparrow+N^\downarrow$, as a measure of the electron spin polarization we define $\Delta N=N^\downarrow-N^\uparrow/2$. From the above selection rules for circularly polarized light, the polarization (σ^\pm) dependent absorption coefficient can be arrived at from a simple modification of Eq. (1), viz.,

$$\alpha^\pm(\omega, N, \Delta N) = a_0 \sum_{v,c} \mu_v^{3/2} S_c^\pm C_{v,c}(\omega, N, \Delta N) \sqrt{\Delta E_c(N, \Delta N)} \times [1 - f_v(k_v) - f_c(k_v)], \quad (2)$$

where the c refers to the different (spin) conduction bands. Here $S_\uparrow^+ = S_\downarrow^- = 1/4$ and $S_\uparrow^- = S_\downarrow^+ = 3/4$ as indicated in Fig. 2. We have implicitly included the possibility that many-body effects depend on spin density through ΔN since different occupancies of the $|\uparrow\rangle$ and $|\downarrow\rangle$ conduction bands lead to different shifts of those band edges and associated band gaps, E_g^\uparrow and E_g^\downarrow . In general one can expect that the energy of the $|\uparrow\rangle$ or $|\downarrow\rangle$ bands will be related to their occupancy so that ΔE_c reflects these occupancies with $\Delta E_\uparrow(N, \Delta N) = \hbar\omega - E_g^\uparrow(N, \Delta N)$ and, by symmetry, $\Delta E_\downarrow(N, \Delta N) = \hbar\omega - E_g^\downarrow(N, -\Delta N)$. The Coulomb enhancement factors $C_{v,c}(\omega, N, \Delta N)$ generally should also reflect spin imbalance and, as with the $\Delta E_\uparrow(N, \Delta N)$ terms, one can expect $C_{v,\uparrow}(\omega, N, \Delta N) = C_{v,\downarrow}(\omega, N, -\Delta N)$. There is a vast literature which discusses carrier many-body effects such as the spin-insensitive correlation effects and the spin-sensitive exchange effects. However, the spin dependence is not often explicitly discussed, and, usually the different spin states are simply summed over. We include the possibility of this spin dependence here, and indeed it is essential for our analysis, although it is beyond the scope of this paper to attempt an explicit calculation of the magnitude of the spin-dependent many-body effects.

We define the differential transmission as $\Delta T/T = (T' - T)/T$ where $T'(T)$ is the probe transmission with (without) the pump beam. Except in cases where a high density of carriers is present and probing occurs near the band edge, the change in refractive index, and hence the change in reflectivity of the semiconductor is small so that ΔT is dominated by changes in the absorption coefficient. In cases where $\Delta T \ll T$ one has $\Delta T/T = -\Delta\alpha^\pm L$, where $\Delta\alpha^\pm$ is the change in absorption coefficient experienced by the σ^\pm -polarized probe beam whose quiescent value is α_0^\pm . The differential absorption can then be approximately written as the sum of terms related to phase space filling and many-body effects so that,

$$\Delta\alpha^\pm = (\Delta\alpha^\pm)_{\text{PSF}} + (\Delta\alpha^\pm)_{\text{MB}}, \quad (3)$$

where

$$(\Delta\alpha^\pm)_{\text{PSF}} \approx -a_0 \sum_{v,c} \mu_v^{3/2} S_c^\pm C_{v,c}(\omega, N, \Delta N) \sqrt{\Delta E_c(N, \Delta N)} \times [f_v(k_v) + f_c(k_v)] \quad (4)$$

and

$$(\Delta\alpha^\pm)_{\text{MB}} = a_0 \sum_{v,c} \mu_v^{3/2} S_c^\pm \Delta [C_{v,c}(\omega, N, \Delta N) \sqrt{\Delta E_c(N, \Delta N)}]. \quad (5)$$

Many-body induced changes in the CEF and BGR are considered together as was done by Langot *et al.*⁴ so that $\frac{\Delta [C_{v,c}(\omega, N, \Delta N) \sqrt{\Delta E_c(N, \Delta N)}]}{\sqrt{\Delta E_c(N, \Delta N)} - C_{v,c}(\omega, 0, 0) \sqrt{\Delta E_c(0, 0)}} = C_{v,c}(\omega, N, \Delta N) \sqrt{\Delta E_c(N, \Delta N)} - C_{v,c}(\omega, 0, 0) \sqrt{\Delta E_c(0, 0)}$. In general, with increasing N the many-body term increases so that $(\Delta\alpha^\pm)_{\text{MB}}$ is positive, whereas increasing N makes $(\Delta\alpha^\pm)_{\text{PSF}}$ negative. Also one can expect that increasing N will reduce the CEF factor, $C_{v,c}(\omega, N, \Delta N)$, due to screening but increase the $\sqrt{\Delta E_c(N, N^\uparrow)}$ factor due to BGR, with the latter dominating.⁴ Using approximations similar to those made by Langot *et al.*, we write the PSF term as

$$(\Delta\alpha^\pm)_{\text{PSF}} \approx -a_0 \sum_{v,c} \mu_v^{3/2} S_c^\pm C_{v,c}(\omega, 0, \Delta 0) \sqrt{\Delta E_c(0, 0)} \times [f_v(k_v) + f_c(k_v)]. \quad (6)$$

Without loss of generality, in what follows we consider the pump beam to always have σ^+ polarization. For a σ^\pm polarized probe beam the differential transmission change is denoted by $(\Delta T/T)^\pm$ from which one can define⁵ a parameter D ,

$$D = \frac{(\Delta T/T)^+ - (\Delta T/T)^-}{(\Delta T/T)^+ + (\Delta T/T)^-}. \quad (7)$$

This parameter directly reflects spin-dependent effects and in those cases where the $(\Delta T/T)^\pm$ varies linearly with N , D is independent of density, and therefore recombination effects.

In carrying out our simulations we have assumed parabolic bands and commonly accepted parameters for GaAs.¹⁹ Figure 3 shows the density dependence of $(\Delta T/T)_{\text{PSF}}^\pm$ for a probe wavelengths of 775 and 855 nm, assuming $N^\downarrow = 3/4N$ as induced initially by the σ^+ pump beam; the carrier and lattice temperature are taken as 295 K. The differential transmission for both wavelengths is dominated by the $f_\downarrow(k_{lh})$ and $f_\uparrow(k_{lh})$ electron Fermi factors at low and high densities with the (unpolarized) hole Fermi terms making only small contributions (cf. Fig. 1 of Langot *et al.*⁴). Over the density range indicated there is a linear variation of the differential transmission with density as expected when the probe beam effectively samples the tail of a Fermi-Dirac distribution. For both wavelengths the calculated D parameter is not less than its maximum possible value of 0.25 by more than a few % over the entire density range; however, for the longer probe wavelength and densities approaching $3 \times 10^{17} \text{ cm}^{-3}$ where electron degeneracy sets in, the heavy hole Fermi factor

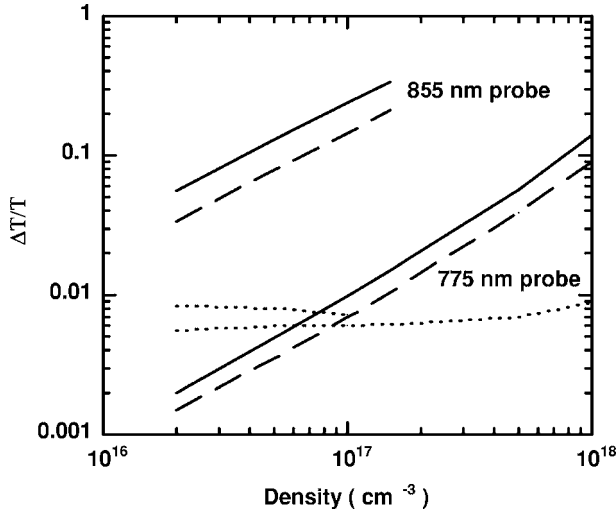


FIG. 3. Simulated differential transmission of GaAs for probe wavelengths of 775 nm and 855 nm; the solid and dashed lines indicate ΔT_{PSF}^+ and ΔT_{PSF}^- for 855 nm and 775 nm, respectively, while the dotted curves show $-\Delta T_{\text{MB}}^+$ at 855 nm (upper curve) and 775 nm (lower curve) for spin unpolarized electrons.

$f_{hh}(k_{hh})$ causes D to decrease slightly. For all densities, with $N^\downarrow = 3/4N$, we find, as expected, that $(\Delta T/T)_{\text{PSF}}^+ > (\Delta T/T)_{\text{PSF}}^-$.

To frame the discussion of the influence of many-body effects on transmissivity in Fig. 3 we show the calculated $(-\Delta T/T)_{\text{MB}}^\pm$ for 855 and 775 nm probe wavelengths as a function of carrier density at room temperature assuming no net spin polarization [$N^\uparrow = N^\downarrow = N/2$, for which $(\Delta T/T)_{\text{MB}}^+ = (\Delta T/T)_{\text{MB}}^-$]. Note that the electron Fermi level enters the conduction band near $N \approx 3 \times 10^{17} \text{ cm}^{-3}$ and that for the 855 nm probe, the approximation of $\Delta T/T \ll 1$, breaks down. We assume that the band-gap renormalization is, as given by Bennett *et al.*,²⁰ $-10 \text{ meV} (N/10^{17} \text{ cm}^{-3})^{1/3}$ but allowing for band-gap renormalization to exist below $5 \times 10^{16} \text{ cm}^{-3}$. Other functional forms (within reason) may be used but the choice does not substantially alter the discussion that follows; also, we do not wish to place undue emphasis on the exact transmission values calculated here considering the approximations made. The main point, as can be seen in Fig. 3, is that for a probe photon energy near the band gap the influence of many-body effects on the differential transmission is much smaller and of opposite sign to that from phase-space filling. However, for the higher probe energy many-body and phase space filling effects apparently make comparable contributions albeit of opposite sign to the differential transmission at low carrier densities with the relative importance of many-body effects decreasing with increasing density. For a spin imbalance, e.g., $N^\downarrow > N^\uparrow$, because of the expected larger band-gap renormalization for the $|\downarrow\rangle$ states than for the $|\uparrow\rangle$ states one might expect $|(\Delta T/T)_{\text{MB}}^+| > |(\Delta T/T)_{\text{MB}}^-|$ and so it will be possible for $(\Delta T/T)^+ < (\Delta T/T)^-$. Hence, spin-dependent many-body effects not only reduce the value of D but even change its sign. We will use a sign change of D as indicative of spin-dependent many-body effects.

It should be emphasized that the above discussion serves as a guideline for the experimental results that follow. Many-

body effects, especially for nondegenerate carrier distributions, are difficult to calculate with any confidence and there still remains considerable speculation on various aspects of such calculations such as whether band-gap renormalization leads to a rigid shift of bands and exactly what the dependence on excess carrier density is, both for impurity doped semiconductors as well as optically pumped semiconductors.^{21,22} In addition there are several other approximations used above related to parabolic, isotropic bands, etc. In what follows, in view of all these uncertainties and approximations we adopt a conservative approach and only offer semiquantitative remarks and conclusions.

III. EXPERIMENT

Polarization-resolved differential transmission measurements were carried out by pump-probe techniques using femtosecond pulses from an infrared optical parametric amplifier (OPA) pumped by a regeneratively amplified Ti:sapphire laser operating at 250 kHz. Signal (or idler) pulses are frequency doubled in a beta barium borate (BBO) crystal generating $\sim 150 \text{ fs}$ pulses with a bandwidth of $\sim 30 \text{ meV}$ and tunable between 660 nm and 1050 nm. Probe pulses are derived from pump pulses using a 10–90 % beamsplitter. The polarization and intensity of each pulse are separately controlled using wave plates and polarizers. The probe pulses are delayed from the pump pulses using a retroreflector mounted on a motorized translation stage. The two beams are then focused with the same lens onto the sample with the probe beam normally incident while the pump beam propagation direction makes an angle of 10° with the normal. The pump and probe beam each have a spot size (full-width at half-maximum) of approximately $60 \mu\text{m}$. The probe transmitted signal is measured with a silicon detector behind the sample.

The sample is a semi-insulating $1 \mu\text{m}$ thick (100) oriented bulk GaAs (with impurity concentration $< 10^{15} \text{ cm}^{-3}$) that was van der Waals bonded to a glass substrate. The pump fluence, F , used in the experiments is in the range $1.3 \mu\text{J cm}^{-2} < F < 50 \mu\text{J cm}^{-2}$; the probe fluence in all experiments is no more than $0.1F$. All measurements were performed at room temperature. Note that although we quote center wavelengths, the differential transmission for pulses can also reflect the pulse bandwidth. In particular since transmission bleaching effects vary with the Fermi occupancy factors which vary exponentially with carrier energy, the effective probe wavelength is slightly ($< 5 \text{ nm}$ in our case) below the probe pulse center wavelength.

For a given pump fluence we can estimate the excited carrier density taking into account two averaging effects. First, the sample thickness is comparable to the pump absorption depth of $\sim 1 \mu\text{m}$. The carrier density on the back surface is therefore $\sim e^{-1}$ of its value of the front surface. Moreover, the probe spot size is comparable to that of the pump spot so that the carrier density being probed varies across the probe spot. When both factors are considered the average density probed, N , is ~ 0.4 of the peak carrier density which is estimated as $(1-R)\alpha F/\hbar\omega_p$ where α is the pump absorption coefficient, $\hbar\omega_p$ is the pump photon energy

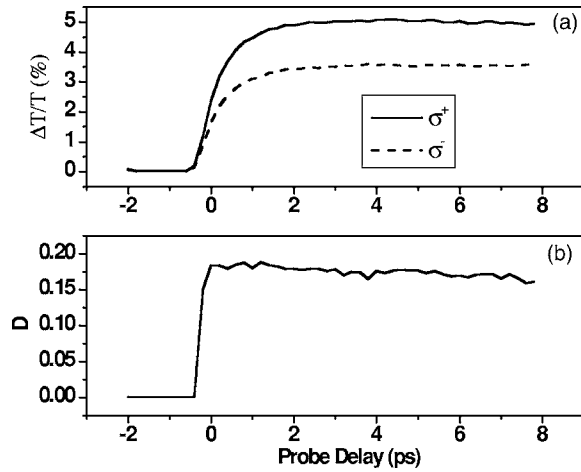


FIG. 4. (a) Differential transmissivity for σ^+ (solid curve) and σ^- (dashed curve) 855 nm probe pulses as a function of time delay from a 775 nm σ^+ polarized pump pulse with a fluence $6.3 \mu\text{J cm}^{-2}$; (b) time dependence of D for the same data.

and R is the sample reflectivity. For our range of pump fluence N is between $2 \times 10^{16} \text{ cm}^{-3}$ and $\sim 10^{18} \text{ cm}^{-3}$.

IV. RESULTS AND DISCUSSION

Figure 4(a) shows the differential transmission for σ^+ and σ^- 855 nm probe pulses as a function of time delay from a 775 nm σ^+ polarized pump pulse with a fluence of $F = 6.3 \mu\text{J cm}^{-2}$ producing a carrier density, N , of $1.3 \times 10^{17} \text{ cm}^{-3}$. The probed electron average kinetic energy is $\sim 20 \text{ meV}$. Both ΔT^+ and ΔT^- rise on a time scale of about 0.5 ps following the excitation pulse, essentially the cooling time of the electrons and holes¹ during which the occupancy of electrons in the probed states increases; note that ΔT^+ is always $> \Delta T^-$. Consistent with the simulations depicted in Fig. 3 both differential transmission traces reflect phase space filling for the experimentally estimated carrier density. The experimental and theoretical values of the absolute transmissivity differ, but this is not surprising in view of the approximations in both the simulations and the estimate of the experimental carrier density. As shown in Fig. 4(b) the extracted D parameter rises on a pump pulse-width related time scale to the constant value of 0.18, near the value of 0.25 expected for $N^{\downarrow} = 3/4N$, with phase space filling alone determining the transmission behavior. The discrepancy between the measured value of ~ 0.18 and 0.25 value likely reflects the influence of hole Fermi factors and a small contribution from many-body effects.

Figure 5 shows the results of a similar experiment with an 855 nm pump of fluence $25 \mu\text{J cm}^{-2}$ (with $N \sim 3 \times 10^{17} \text{ cm}^{-3}$) and probe wavelength of 775 nm for which the probed electron kinetic energy is 90 meV for electrons excited from the lh band and 160 meV for electrons excited from the hh band. Figure 5(a) shows the measured $\Delta T/T^+$ and $\Delta T/T^-$ as a function of delay time while Fig. 5(b) shows the corresponding D parameter extracted from the same data. The differential transmission becomes negative during the pump pulse at which time most of the carriers have not yet

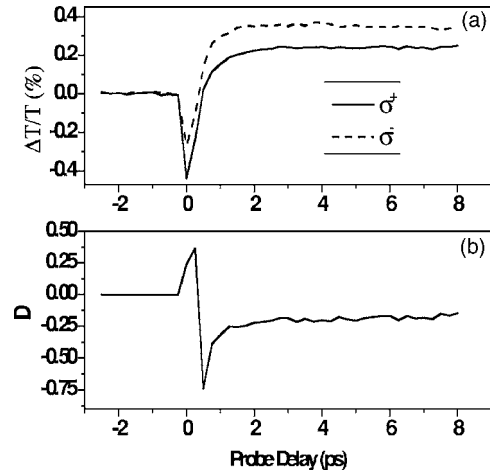


FIG. 5. (a) Differential transmissivity for σ^+ (solid curve) and σ^- (dashed curve) 775 nm probe pulses as a function of time delay from a 855 nm σ^+ pump pulse with a fluence $25 \mu\text{J cm}^{-2}$; (b) extracted time dependence of D .

thermalized with the lattice so as to allow the electrons to occupy the optically probed conduction band states at higher energy. The presence of a negative signal indicates that many-body effects do occur during the pump pulse (e.g., band-gap reduction alone would account for an increase in the absorption coefficient or decrease in transmission) since phase space filling always gives $(\Delta T/T)_{\text{PSF}}^{\pm} > 0$. This behavior is similar to that observed by Langot *et al.* for linearly polarized pump and probe pulses.⁴ However, what is also clearly evident from the σ^+ and σ^- transmission data is that there is a spin dependence of the many-body effects. Following the dip in transmission, as the electrons thermalize by absorbing phonons from the lattice on a 0.5 ps time scale, the Fermi factors increase at the probe energy and the differential transmission increases as phase space filling competes with and eventually dominates many-body effects in determining the overall value of the transmissivity. However, with increasing probe delay following pump induced transient effects, the $\Delta T/T^+$ signal drops below the $\Delta T/T^-$ value and the D parameter becomes negative, attaining a value of about -0.3 .

Figure 6(a) shows the results of similar experiments but with a $6.3 \mu\text{J cm}^{-2}$ from a 775 nm pump pulse and a 775 nm probe pulse. In this case with the electrons establishing a temperature of hundreds of degrees during the pulse, phase space filling contributions to $\Delta T/T^{\pm}$ peak during the pulse and then decay with a time constant of $\sim 0.5 \text{ ps}$, the carrier cooling time. Figure 6(b) shows the value of D extracted from the data; after several picoseconds D becomes negative with approximately the same value as observed in Fig. 5(b). In a separate experiment, the pump beam was linearly polarized (an equal superposition of σ^+ and σ^- , producing equal populations of up and down spins) and the sample transmission was probed with σ^+ and σ^- pulses. The extracted D parameter is indistinguishable from zero as indicated in Fig. 6(b). As illustrated in the theoretical section, many-body effects are expected to reduce the differential transmissivities, and in the absence of spin effects, would do so by the same

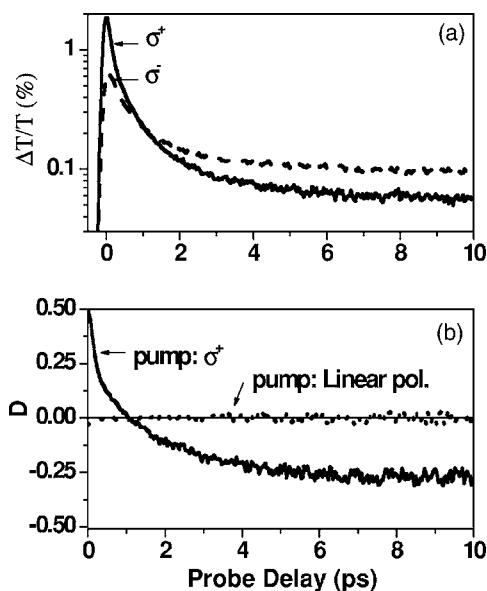


FIG. 6. (a) Differential transmissivity for σ^+ (solid curve) and σ^- (dashed curve) 775 nm probe pulses as a function of time delay from a 775 nm σ^+ pump pulse with a fluence $6.3 \mu\text{J cm}^{-2}$; (b) extracted time dependence of D for data in (a) as well as from experiments which employed a linearly polarized pump pulse.

amounts. The observation that $(\Delta T/T)^+$ drops below $(\Delta T/T)^-$ indicates that the imbalance in the electron spin population with $N^\downarrow > N^\uparrow$ reduces the one differential transmission more than the other and so $\Delta[C_{v,\downarrow}(\omega, N, \Delta N)\sqrt{\Delta E_\downarrow(N, \Delta N)}] > \Delta[C_{v,\uparrow}(\omega, \Delta N,) \times \sqrt{\Delta E_\uparrow(N, \Delta N)}]$. This would be possible, e.g., if the $|\downarrow\rangle$ bands experience larger band-gap reduction than the $|\uparrow\rangle$ bands, a not unlikely possibility. If one had interpreted D as a measure of the relative spin populations from Fig. 6 one would have concluded incorrectly that the spin polarization evolved on a few ps time scale and indeed changed sign.

A comparison of the results of Fig. 4 with the simulations in Fig. 3 shows that while near-band-edge probing allows one to deduce (albeit approximately) the degree of spin polarization, probing at photon energies well above the band gap is less sensitive to phase space filling effects and increasingly sensitive to many-body effects. Indeed, one probes both the net electron spin population and the spin-dependent many-body effects.

To further emphasize the dependence of the D parameter on the carrier density as well as the probing wavelength, we have carried out experiments in which either the pump fluence was varied or the probe wavelength was varied. Figure 7 shows D as a function of the time delay between 775 nm pump and probe pulses for four different pump fluences, *viz.*, $F = F_0, 2F_0, 4F_0, 8F_0$ where $F_0 = 6.3 \mu\text{J cm}^{-2}$ which yield average carrier densities between $1.3 \times 10^{17} \text{ cm}^{-3}$ and $1.0 \times 10^{18} \text{ cm}^{-3}$. As observed in Figs. 5 and 6, at the lowest fluence D is negative for delay times longer than 1 ps, however it becomes increasingly positive as F and the carrier density increases. With reference to Fig. 3, one sees that phase space filling effects are expected to increase linearly with density, whereas many-body effects have a sublinear dependence and become less important at higher densities.

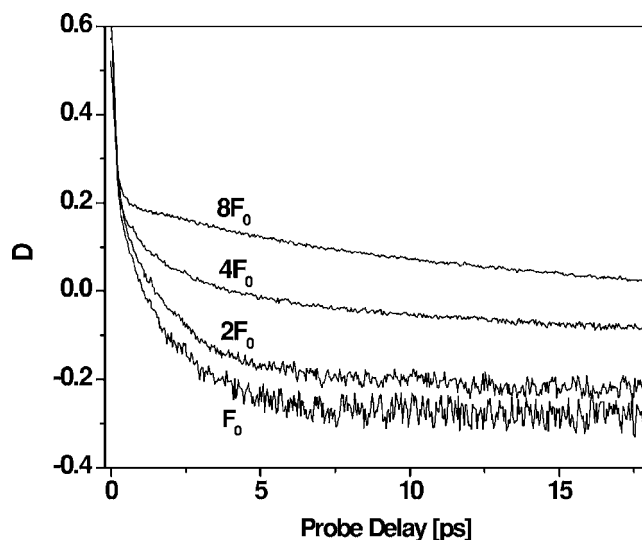


FIG. 7. Dependence of D on delay between 775 nm pump and probe pulses for different pump fluence with $F_0 = 6.3 \mu\text{J cm}^{-2}$.

Hence with increasing carrier density the value of D is expected to approach the results shown in Fig. 4. The decay of the D parameter on a 3 ps time scale (longer than the carrier cooling time) at the two lower fluences partly reflects crossover effects in the differential transmission time evolution as noted above. At the higher fluences the increasing decay time reflects spin relaxation and evolution of the many-body components of the differential transmission as the spin populations equilibrate.

Figure 8 shows a plot of D as a function of probe delay between σ^+ and σ^- degenerate pump and probe pulses at 865, 800, and 775 nm with a pump fluence of 1.26, 3.15, and $6.3 \mu\text{J cm}^{-2}$ for which the peak carrier densities are $2 \times 10^{16} \text{ cm}^{-3}$, $6 \times 10^{16} \text{ cm}^{-3}$, and $1.3 \times 10^{17} \text{ cm}^{-3}$. As the energy of the probed electrons decreases, D is observed to increase, changing from negative to positive, becoming near zero, and virtually time independent, at the probe wavelength

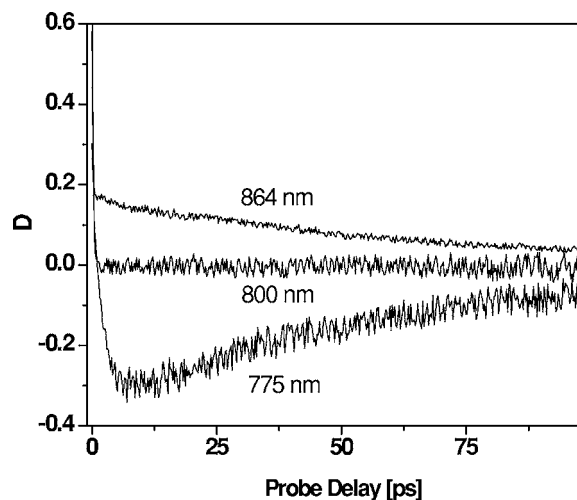


FIG. 8. Dependence of D on delay between wavelength degenerate pump and probe pulses at 864, 800, and 775 nm with a pump fluence of 1.26, 3.15, and $6.3 \mu\text{J cm}^{-2}$.

of 800 nm, where apparently the spin-sensitivity components of the many-body and phase space filling effects nearly compensate each other. At the probe wavelengths of 865 and 775 nm D decays to zero with the same decay time of ~ 65 ps reflecting spin relaxation. From the measured 65 ps decay time of the transmissivity we deduce that the spin relaxation time is 130 ps.

V. CONCLUSIONS

We have presented experimental results of differential transmission measurements of GaAs at 295 K using circularly polarized 150 fs pump and probe pulses to examine the role of electron spin at different carrier densities and probed at different photon energies above the fundamental band gap. Our results can be explained in terms of spin-sensitive phase-space filling and many-body effects. For probing near the band-edge, the transmissivity results are well explained in terms of phase-space filling, dominated by the electron contribution to semiconductor bleaching, with many-body effects playing a minor role. For probing of spin polarized electrons with larger photon energies, many-body effects become increasingly important and compete with phase space filling to determine the overall transmissivity of GaAs. This allows us to examine the spin dependence of the many-body

effects, essentially by probing the tail of the electron distribution. Our observations are semiquantitative at this time, partly because of the usual experimental uncertainties for the carrier densities, and await a suitable model for spin-dependent band-gap renormalization and the Coulomb enhancement factor. However, we do note that the electron spin relaxation time is about 130 ps consistent with the work of others. Future work might consider measurements over a wider range of densities and initial polarization conditions, and theoretical models which might provide a quantitative foundation for our results. Finally, we note that if one does not take account of these spin-sensitive many-body effects in optical probing of spins in semiconductor one can misinterpret both the magnitude of the spin polarization, as well as its time evolution, especially if recombination occurs on the same time scale as spin relaxation.

ACKNOWLEDGMENTS

This work was supported in part by the Sciences and Engineering Research Council of Canada, Photonics Research Ontario, the Defense Advanced Research Projects Agency and the Office of Naval Research. The authors gratefully acknowledge stimulating discussions with J. Sipe, I. Rumyantsev, E. Sherman, and R.D.R. Bhat.

*Present address: Charles University in Prague, Faculty of Mathematics and Physics, Ke Karlovu 3, 121 16 Prague 2, Czech Republic.

¹J. Shah, *Ultrafast Spectroscopy of Semiconductors and Semiconductor Nanostructures*, 2nd ed., Springer Series in Solid State Science, Vol. 115 (Springer, Berlin, 1999).

²H. Haug and S. W. Koch, *Quantum Theory of the Optical and Electronic Properties of Semiconductors*, 2nd ed. (World Scientific, Singapore, 1993).

³P. C. Becker, H. L. Fragnito, C. H. Brito Cruz, R. L. Fork, J. E. Cunningham, J. E. Henry, and C. V. Shank, *Phys. Rev. Lett.* **61**, 1647 (1988).

⁴P. Langot, R. Tommasi, and F. Valleé, *Phys. Rev. B* **54**, 1775 (1996).

⁵J. T. Hyland, G. T. Kennedy, A. Miller, and C. C. Burton, *Semicond. Sci. Technol.* **14**, 215 (1999).

⁶D. Awschalom and J. Kikkawa, *Phys. Today* **52**, 33 (1999).

⁷S. Wolf *et al.*, *Science* **294**, 1488 (2001).

⁸B. P. Z. F. Meyer, *Optical Orientation*, Modern Problems in Condensed Matter Science (North-Holland, Amsterdam, 1984).

⁹B. P. Zakharchenya, D. N. Mirlin, V. I. Perel', and I. I. Reshina, *Usp. Fiz. Nauk* **136**, 459 (1982) [*Sov. Phys. Usp.* **25**, 143

(1982)].

¹⁰R. Seymour and R. Alfano, *Appl. Phys. Lett.* **37**, 231 (1980).

¹¹D. Pierce and F. Meier, *Phys. Rev. B* **13**, 5484 (1976).

¹²J. Hyland *et al.*, *Semicond. Sci. Technol.* **14**, 215 (1999).

¹³A. Alexandrou, V. Berger, and D. Hulin, *Phys. Rev. B* **52**, 4654 (1995).

¹⁴A. Tackeuchi, Y. Nishikawa, and O. Wada, *Appl. Phys. Lett.* **68**, 797 (1996).

¹⁵D. J. Hilton and C. L. Tang, *Phys. Rev. Lett.* **89**, 146601 (2002).

¹⁶Y. Lee *et al.*, *Phys. Rev. Lett.* **57**, 2446 (1986).

¹⁷J. P. Lowenau, F. M. Reich, and E. Gornik, *Phys. Rev. B* **51**, 4159 (1995).

¹⁸W. Schaefer and M. Wegner, *Semiconductor Optics and Transport* (Springer-Verlag, New York, 2002).

¹⁹*Semiconductors-Basic Data*, edited by O. Madelung (Springer, New York, 1996), p. 101.

²⁰B. R. Bennett, R. A. Soref, and J. A. Del Alamo, *IEEE J. Quantum Electron.* **26**, 113 (1990).

²¹G. Trankle, H. Leier, A. Forchel, H. Haug, C. Ell, and G. Weimann, *Phys. Rev. Lett.* **58**, 419 (1987).

²²R. Blank and H. Haug, *Phys. Rev. B* **44**, 10513 (1991).